Original Research Article Nanotechnology

International Journal of Pharma and Bio Sciences

ISSN 0975-6299

LOCALIZATION AND UPTAKE OF FLUORESCENTLY LABELLED GOLD NANOPARTICLES BY A T47D HUMAN BREAST CANCER CELL LINE

ZAHRAH ALHALILL[1], ABEER ZAILA[2], BARBARA SANDERSON[2], JOE SHAPTER[*1]

[1]Flinders Centre for NanoScale Science and Technology, School of Chemical and Physical Sciences, Flinders University, Adelaide, SA 5001, Australia
[2]Medical Biotechnology, School of Medical Science and Technology, Flinders University, Adelaide, SA 5001, Australia

ABSTRACT

Finding new cancer treatments based on novel drug delivery approaches is critically important.Gold nanoparticles (AuNPs) for use in drug delivery and cellular imaging were functionalized using a two-step synthesis method using modified carboxylic terminated alkane-thiols to attach fluorescent dyes (DAPI or $pyNH_2$) to the carboxylic ends of the thiolated AuNPs.The cellular cytotoxicity showed that the fluorescently labelled AuNPs were non-toxic at low concentrations.Confocal laser scanning microscopy (CLSM) showed an efficient internalization and uptake of AuNPs by T47D breast cancer cells within 1 hour of incubation.The fluorescence intensity increases over time for both conjugates.When conjugating DAPI with gold nanoparticles, the behaviour is quite different from free DAPI.TEM results showed the localization of AuNPs in the cytoplasm, the cell periphery and near the perinuclear region.The surface chemistry of AuNPs plays an important role in facilitating their cellular uptake as TEM images for conjugates containing DAPI show more AuNPs were internalized by the cells.These various forms of imaging give a clear insight into how these potential drug carriers interact with cells and are subsequently adsorbed into the cells.These are the core processes that will determine if the drug delivery approaches will ultimately be successful.

KEYWORDS: *Gold nanoparticles, Fluorescent agents, Intracellular uptake*

JOE SHAPTER *

Flinders Centre for NanoScale Science and Technology, School of Chemical and Physical Sciences, Flinders University, Adelaide, SA 5001, Australia

***Corresponding Author**

Received on: 05.07.2016
Revised and Accepted on: 23.01.2017
DOI: http://dx.doi.org/10.22376/ijpbs.2017.8.1.p260-269

INTRODUCTION

The latest advances in nanotechnology open the door to use a variety of nanoparticles, including metallic nanoparticles, in a wide range of biomedical applications such as diagnostic imaging or drug delivery for cancer therapy.[1, 2] The use of gold nanoparticles as a platform for cell imaging, gene and drug delivery and therapy in nanomedicine applications has attracted great attention due to the unique physical, biological and chemical properties of the particles.Gold nanoparticles show no inherent cytotoxicity against human cells, can be synthesized in different sizes and shapes easily, their surface can be easily functionalized with different biomolecules, they show high stability and they are biocompatible.[3-5] Current research is focused on the interactions between gold nanoparticles (AuNPs) and mammalian cells, strategies of cellular uptake, the fate of AuNPs inside the cell and their removal from the cells then from the body.[6] The cellular uptake of the AuNPs is highly dependent on different factors including the particle's size, shape and the surface functionalization.[6] Functionalization of the surface of gold nanoparticles is a prerequisite for biological and medical applications as the added functionalization can be used to specifically interact with the cells or other biomolecules such as chemotherapeutic agents[7] or antibodies.[8] Many studies have used thiol compounds to modify the AuNP surface.[9-13] Negatively charged or neutral AuNPs show a longer circulation time.[14] Functionalization of the AuNP surface through short chains exchanged by long chain alkane-thiols provides a stable system allowing the functionalized particles to remain in circulation system for longer periods of time.[15] Conjugation of fluorescent probes to different molecules including ligand functionalized nanoparticles surfaces is an important application to track, image and investigate the nanoparticle fate inside cells which helps to understand the interactions between those particles and cells thus improving their effectiveness for diagnosis and treatment of diseases.Attachment of dyes to functionalized AuNPs can facilitate tracking the gold particles inside cells.[16] For example, AuNPs can be detected by fluorescence either by attachment of a fluorescent probe to the AuNPs or through a fluorescent gold core.[17, 18] Fu et al.[2] attached Coumarin dye to the surface AuNPs through a PEG-thiol ligand.It was found that the prepared conjugate was dramatically fluorescent.This can be attributed to the distance between the gold particle and Coumarin dye through using a PEG-thiol spacer being large enough to avoid the fluorescence quenching effect of AuNPs.[2, 19] Moreover, these nanoparticles were nontoxic to MDA-MB-231 breast cancer cells according to a cytotoxicity assay and the functionalized AuNPs were internalized by the tumour cells after one hour of incubation by non-specific endocytosis and they localized in the cytosol and perinuclear area.[2] DAPI, 2-(4-Amidinophenyl)-6-indolecarbamidine dihydrochloride, 4′,6-diamidino-2-phenylindole dihydrochloride, is a fluorescent dye.It is commonly used for staining DNA molecules producing a stable complex with more intense fluorescence than DAPI alone.[20, 21] The binding of DAPI onto DNA occurs because the nitrogen in the indole in DAPI structure develops a bifurcated hydrogen bond with A-T regions in DNA.[21] DAPI can be used for other life science applications.[22] For example, Rudershausen et al.[23] reported the covalent attachment of fluorescent dye, DAPI, dichlorotriazinyl derivative, DTAF, or rhodamine B, onto the surface of the dextran coated superparamagnetic iron oxide nanoparticles.In their study, they used bifunctional carboxylic acid as a spacer to link the fluorescent dye via one of its amino groups to hydroxyl groups of the dextrancoatediron oxidenanoparticles.Since dextran has many functionalities (–OH), biomolecules, such as antibodies or proteins, can be covalently bound to the already fluorescently labelled dextran which can be used as nanocarrier system.[23] 1-Pyrenemethylamine hydrochloride, $pyNH_2$, has been used in different biomedical applications.For example, Yang et al.[24] used $pyNH_2$ to prepare functionalized graphene oxide (GO) by conjugation of polyethylene glycol (PEG) and folic acid (FA), followed by the loading of human telomerase reverse transcriptase (hTERT) small interfering RNA (siRNA) with an assistance of 1-pyrenemethylamine hydrochloride through π–π stacking onto the surface of GO.This system was designed for tumour targeting delivery of siRNA.It was found that after loading $pyNH_2$, the PEG functionalized GO was non-toxic.[24] This finding does suggest that fluorescent $pyNH_2$ could be used as a probe for AuNP detection inside the cells *in vitro* system.Another study conducted by Lodeiro et al.[25] has shown the synthesis of new $pyNH_2$ derivatives by binding of two $pyNH_2$ units to the carbonyl precursor 2,6-bis(2-formylphenoxymethyl) pyridine.In this study, two biscromophoric sensors and one monochromophoric system based on pyrene emission were synthesized to be used for selective fluorescence sensing applications.[25] In this study, we describe the cellular cytotoxicity evaluation of fluorescently labelled AuNPs to optimise the safe concentration of the fluorescent probes used for intracellular tracing and imaging of AuNPs.We used confocal laser scanning microscopy (CLSM) and transmission electron microscopy (TEM) to study the localization and intracellular behaviour of these functionalized AuNPs.The novelty of this research is functionalization of surface of AuNPs by (±)-α-Lipoic acid (LA) as an intermediate for further functionalization to control the kinetics followed by exchange with the long chain 16-mercaptohexadecanoic acid (16-MHDA) to increase the stability of functionalized AuNPs.Such a two step functionalization method to link fluorescent agents with gold nanoparticles has not been reported.The long chain will increase the AuNP circulation time in biological systems by covering the surface to avoid serum protein binding.[26] Covalent attachment of fluorescent stains (DAPI or $pyNH_2$) onto the surface of AuNPs was done via EDC/NHS chemistry.DAPI conjugated (covalently or non-covalently) to AuNPs to detect the fate of AuNPs inside cells has not been reported previously.Choosing these dyes as probes to evaluate their potential cytotoxicity or safety for biomedical applications is important for future work.

MATERIALS AND METHODS

All chemicals and reagents were used as received without any further purification.Gold (III) chloride

trihydrate, paclitaxel, (±)-α-Lipoic acid (LA), 16-mercaptohexadecanoicacid (16-MHDA), Tween® 20, N-(3-Dimethylaminopropyl)-N′-ethylcarbodiimide hydrochloride (EDC), N-Hydroxysuccinimide (NHS),2-(4-Amidinophenyl)-6-indolecarbamidine dihydrochloride (DAPI),1-Pyrenemethylamine hydrochloride were obtained from Sigma Aldrich, Australia.Trisodium citrate dehydrate was purchased from Ajax Finechem Pty Ltd, Australia.Millipore Milli Q water with resistivity = 18.2 MΩ cm was used for all the experiments.Thestocksolution of Taxol was 5mg/mL in DimethylSulfoxide(DMSO).

(i) Synthesis of Citrate-stabilized Gold Nanoparticles (AuNPs)

Gold nanoparticles were synthesized by sodium citrate reduction of $HAuCl_4$ using the method of Turkevich et al.[27, 28] The average diameter of AuNPs as measured by TEM was approximately 17±4 nm.

(ii) Functionalization of Gold Nanoparticles (AuNPs)

Gold nanoparticles were functionalized by a two-step approach described by Lin et al.with some modifications.[15] Tween® 20, which is used as a surfactant to stabilize the particles by physisorption onto the surface of AuNPs and prevent particle aggregation,[29, 30] was first added to the gold colloids.Then, a solution of (±)-α-Lipoic acid (LA) (0.0028 g) in ethanol (0.4 mL) was added, and the mixture stirred at a mild speed for 18 h at room temperature.Then a solution of 16-mercaptohexadecanoic acid (16-MHDA) (0.0028 g) was added to the mixture with further stirring for 18 h at room temperature.The samples were centrifuged 5 times at 15700 g for 15 min to remove excess thiols.This sample is thiol-AuNPs.

(iii) Conjugation of Stain Agents to Functionalized AuNPs

After the surface functionalization of AuNPs, a solution of N-(3-Dimethylaminopropyl)- N′-ethylcarbodiimide hydrochloride (EDC) and N-Hydroxysuccinimide (NHS) dissolved in ethanol was added to activate the carboxylic acid groups.Then, in order to conjugate 2-(4-Amidinophenyl)-6-indolecarbamidine dihydrochloride (DAPI) or 1-Pyrenemethylamine hydrochloride ($pyNH_2$) dye to thiolatedAuNPs, DAPI (0.0057 M) or $pyNH_2$ (0.037 M) solutions were added to the mixture and further stirred overnight.Then, the resulting samples were centrifuged at 15700 g for 15 min five times to separate the unbounded molecules to obtain DAPI-thiol-AuNPs (Figure1) or $pyNH_2$-thiol-AuNPs conjugates.

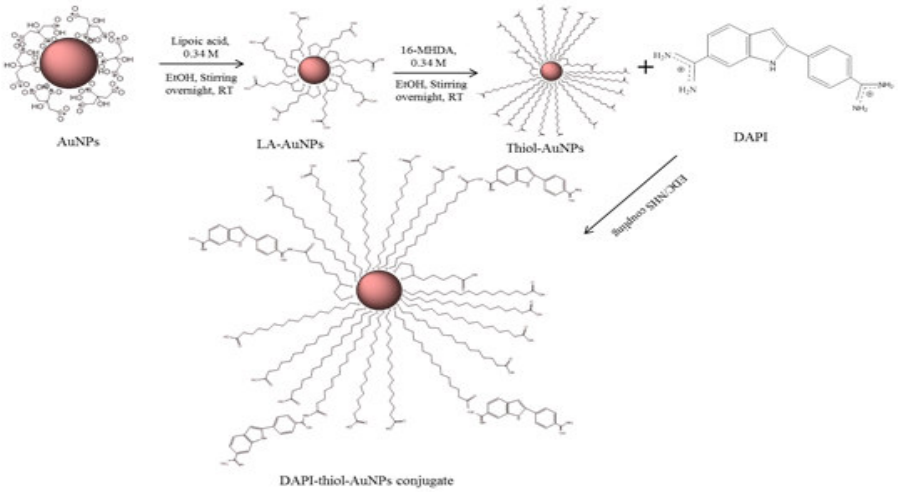

Figure 1
Schematic illustration for chemical synthesis of DAPI-thiol-AuNPs conjugate.
Synthesis for $pyNH_2$is exactly equivalent.

(iv) Nanoparticle Characterization

The prepared conjugates were characterized using a Cary 50UV-vis spectrophotometer (EST 70772) at room temperature, operated at 1 nm resolution.All DLS measurements were taken on the particle analyser-Malvern HPPS.Data was acquired with a scattering angle close to 180 ° at a temperature of 25 °C.Each measurement was run for 2 seconds repeated three times per sample.Fourier transform infrared (FT-IR) spectra were recorded on Perkin Elmer Spectrum 400 FTIR equipped with “Attenuated Total Reflection” (ATR) from MKII Golden Gate, Specac.at a resolution of 2 cm^{-1}.Transmission Electron Microscopy (TEM) characterization was performed using a FEI Tecnai G2 Spirit transmission electron microscope with an accelerating voltage of 100 kV.Image J software was utilized to analyse TEM images.The grids were prepared by depositing a few drops of the sample onto formvar and carbon coated 200 mesh copper grids and then were air dried.A Varian Cary Eclipse Fluorescence Spectrophotometer was used to collect the excitation and emission spectra in the range between 200 and 600 nm.The measurements were carried out using a quartz cuvette (2 mL, 10 mm path length).For all the samples, a baseline correction was performed using Milli-Q water.

(v) CLSM for Intracellular Imaging of AuNPsDistribution

A Leica TCS SP5 scanning confocal microscope equipped with 405 nm, 488 nm and 561 nm diode lasers using LASAF software and a water immersion objective (Leica Biosystems, Australia) was used for cellular

imaging.The single optical sections were recorded collecting an average of 3 images using a 63x magnification lens.Optical sectioning was performed and 3D-images generated with pinhole size set at 1 array unit.Confocal laser imaging was accomplished using the 405 nm diode laser.Although the excitation wavelengths for both DAPI and $pyNH_2$ are less than 400 nm in ultraviolet region, the conjugate could be imaged using 405 nm excitation wavelength as the width of the excitation peaks for the probe provided enough absorption to excite the molecules using this laser wavelength (405 nm).The emitted fluorescence was detected by a photomultiplier tube (PMT).

(vi) Cell Culture

Human ductal breast epithelial tumour cell lines (T47D) were used in the bioassays and obtained from the American Type Culture Collection (ATCC) and supplied by Flinders Medical Centre.The cell lines were grown in 1640 RPMI media, with 10% foetal bovine serum (FBS) and penicillin antibiotics to grow the cell lines.Cells were used every 72-96h after reaching 80% to 90% confluence.The cells were incubated in a completely humidified atmosphere at 37 °C with 5 % CO_2.Cell concentration was estimated by Trypan blue dye exclusion counting involving diluting the cell suspension 1:1 with Trypan Blue dye (TB), then loading the stained cells into a chamber of a Neubauer haemocytometer.Viable and dead cells were counted at Mag 40x using a light microscope.The average number of cells per square was determined then multiplied by the dilution factor (x2) to obtain the viable cell concentration ($x10^6$ cells/ mL).

(vii) Crystal Violet Assay Experimental Procedure

To assess the relative cell survival after exposure to DAPI-thiol-AuNPs and $pyNH_2$-thiol-AuNPs conjugates, a crystal violet assay was carried out in 5 x 96-well flat-bottom plates, one as standard curve and the others as treatment plates (in four replicates).Serial dilutions of cells were prepared in 100µL volume and cells were seeded.T47D was used at the concentration of 2×10^5 cell/well in four replicates.Plates were incubated in a humidified 37 °C, 5% CO_2 incubator for 20-22 h.The following day, medium was removed and 50µL/well of crystal violet stain was placed in standard curve plate and incubated for 10 min at room temperature, prior to washing with Milli-Q (MQ) water.Plates were then left to dry overnight.For treatment plates, cells were treated with 50µL crystal violet mixed with 10 µL of four concentrations of DAPI-thiol-AuNPs (initial concentration of DAPI in the conjugate = 0.0418 mM) and $pyNH_2$-thiol-AuNPs (initial concentration of $pyNH_2$in the conjugate = 0.0073 mM).After 24h, 50 µL of acetic acid was added to each well and the plates were incubated at room temperature for 10 min before reading with a spectrophotometer.

(viii) Intracellular Trafficking Studies Using CLSM

Confocal scanning microscopy was used to monitor intracellular distribution of the labelled gold particles within T47D cells.Samples were prepared via the following methods to measure cell fluorescence.The live cell concentration for the 6-well plate was 0.3×10^5 cells/well.This concentration was seeded and incubated for 20-22 h in a humidified 37°C with 5% CO_2 incubator.Then, plates were treated with 30µL of labelled AuNPs, free DAPI or free $pyNH_2$ solutions (in PBS buffer) diluted with 1.94 mL of RPMI media.The cells were exposed to this mixture for 1 h, 6 h and 24 h.Cell treated coverslips were washed twice with media then cells were harvested and placed carefully in a POC chamber.150µL of fresh media was added to the chamber after sealing and observed under fluorescence microscopy.

(ix) TEM Analysis of Cells Exposed to AuNPs

T47D cells were grown in a 75 cm^2 flask.300µL of the nanoparticle suspension was added to 3mL fresh medium.2 mL of this mixture was added to cells.Cells were incubated in a humidified 37 °C with 5 % CO_2 incubator for 3-4 h.Then, cells were washed using 2mL of media.After that, 1.5mL Trypsin-EDTA was added and incubated for 5-15min.After that, 5 mL of fresh media was added and mixed gently then transferred to 10 mL tube and centrifuged at 1000 rpm for 5min.The media was discarded and the cells were fixed overnight in 500 µL of 4 % paraformaldehyde 1.25% glutaraldehyde in PBS, 4 % sucrose at pH 7.2.The next day, cells were washed in washing buffer once every 5 min (PBS and 4% sucrose).Then, the post fixative step involved addition of 2% OsO_4 for 45 min, followed by dehydration using 70 % ethanol with one ethanol change, 90 % ethanol with two changes, and 100% ethanol with three changes.The next step was resin infiltration using a 1:1 mixture of 100 % ethanol and epoxy resin for 1 h, and 100 % resin for 1h, then 100% resin for another 1h.Cells were embedded overnight in fresh resin.Eventually, cells were polymerized in an oven at 70 ºC for 24 h.

RESULTS

To investigate the localization and cellular uptake of AuNPs, the conjugate DAPI-thiol-AuNPs (or $pyNH_2$-thiol-AuNPs) was synthesized and characterized during each step of preparation.UV-Vis spectroscopy of free DAPI and DAPI conjugated thiol-AuNPs was carried out (Figure 2.A).Likewise, UV-Vis spectra were collected for free $pyNH_2$ and $pyNH_2$ attached thiol-AuNPs.Figure 2.A shows the characteristic absorbance bands of free $pyNH_2$dissolved in DMSO.[24, 31] These absorption bands correspond to the π–π electronic transitions of the aromatic structure electrons of $pyNH_2$ and the absorption values are consistent with other literature.[32-34] Infrared spectra confirming the chemical attachments are provided in the supporting material.Figure 2.B shows TEM images for DAPI-thiol-AuNPs and $pyNH_2$-thiol-AuNPs conjugates, respectively with particle size of approximately 18 nm observed.The particles were spherical with some irregular shapes.Figure 2.C represents the intensity size distribution of DAPI-thiol-AuNPs and $pyNH_2$-thiol-AuNPs conjugates at 50 nm and 45 nm, respectively.The particle size collected by DLS is larger than that recorded by TEM.This difference is due to the fact that DLS measures the hydrodynamic diameter of the sample in solution while the TEM technique provides the size in the absence of a solvent and after the sample is carefully dried.[35] In addition, this difference can be due to the fact that in TEM images,

the highly aggregated particles will not be counted; just the dispersed particles will determine the actual particle size while in DLS the larger particles will be measured and recorded and those larger particles dominate the intensity distribution histograms.[35] The fluorescence excitation and emission spectra from bound dyes were measured.Figure 2.D shows the fluorescence excitation and emission spectra of both conjugates.A strong fluorescence excitation spectrum assigned to DAPI attached thiol-AuNPs was observed at 362 nm.A broad emission peak at approximately 463 nm of DAPI-thiol-AuNPs conjugate dissolved in Milli-Q water at an excitation wavelength of 340 nm was recorded.These observations can be attributed to the interactions and formation of new bonds between DAPI and thiolated AuNPs in the excited state to form the conjugate DAPI-thiol-AuNPs.Similarly, the fluorescence excitation and emission spectra from bound $pyNH_2$ with thiolated AuNPs was recorded (Figure 2.D).

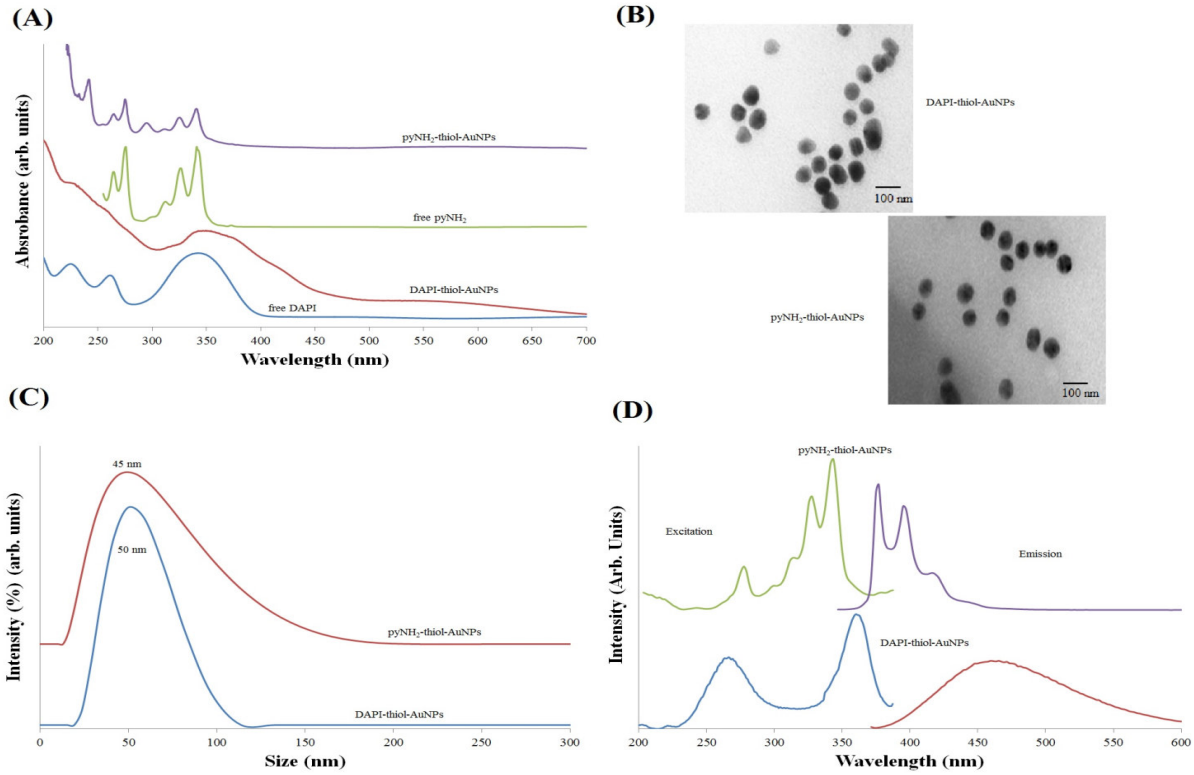

Figure 2

(A) UV-Vis spectroscopy of free staining agents and the conjugates (B) TEM images (C) DLS measurments (D) Fluorescence spectra of the conjugates

Figure 3 shows response of T47D cell line to 24 h treatment with DAPI-thiol-AuNPs or $pyNH_2$-thiol-AuNPs conjugates.The data for cells treated with DAPI containing conjugate shows no extreme reduction of cell relative survival indicating no cytotoxicity.Likewise, the data for cells treated with $pyNH_2$-thiol-AuNPs conjugate shows no significant decrease of cell relative survival in cell lines treated with the concentrations between 3.7 x 10^{-6} and 3.7 x 10^{-4}mM of the conjugate.

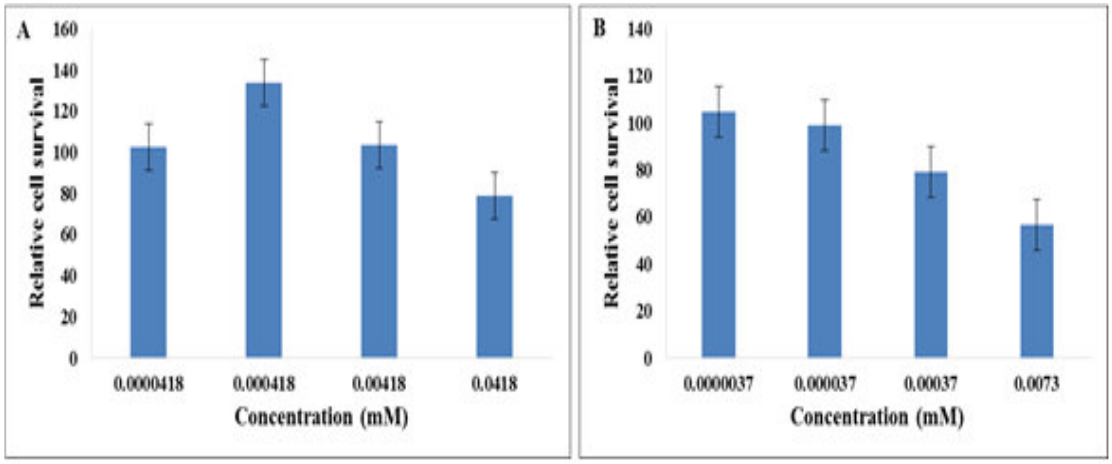

Figure 3

Cytotoxicity analysis of (A) DAPI-thiol-AuNPs (B) $pyNH_2$-thiol-AuNPs conjugate in T47D human breast cancer cells.Results were tested by One-way ANOVA and statistical significance showing * at P < 0.05.

Cellular uptake of 30 µg/mL of free dyes (DAPI or $pyNH_2$) solutions and fluorescently labelled AuNPs was visualized by confocal laser scanning microscopy.Images for T47D cells incubated with free DAPI solutions for 1 h, 6 h and 24 h show DAPI stained the nuclei of the cells as expected.For all exposure times, DAPI accumulated in the nuclei and stained them clearly(Figure 4.a.b and c).Figure 5 shows fluorescence images obtained from cultured T47D cells and incubated up to 24h with 30 µL of each fluorescently labelled conjugate.Overall, both the conjugated nanoparticles were able to internalize and transport across the cell membrane.

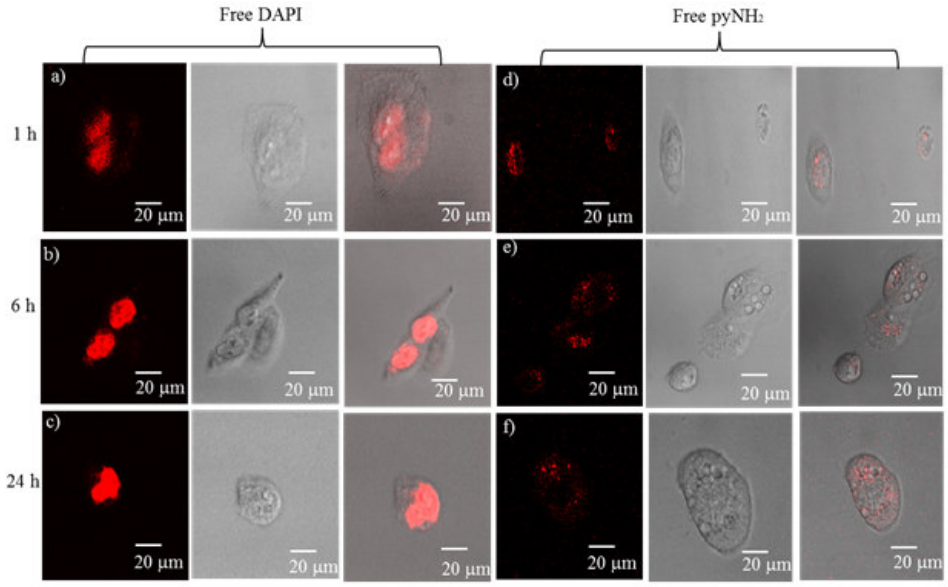

Figure 4

Fluorescence (left) (λ_{ex} = 405 nm, λ_{em} = 478), bright field (middle), and overlaid (right) images of T47D human breast cancer cells treated with free DAPI and free $pyNH_2$ (a, d) after 1 h of incubation (b, e) after 6 h of incubation (c, f) after 24 h of incubation at room temperature.Original magnification was 63×. Scale bars = 20 µm.

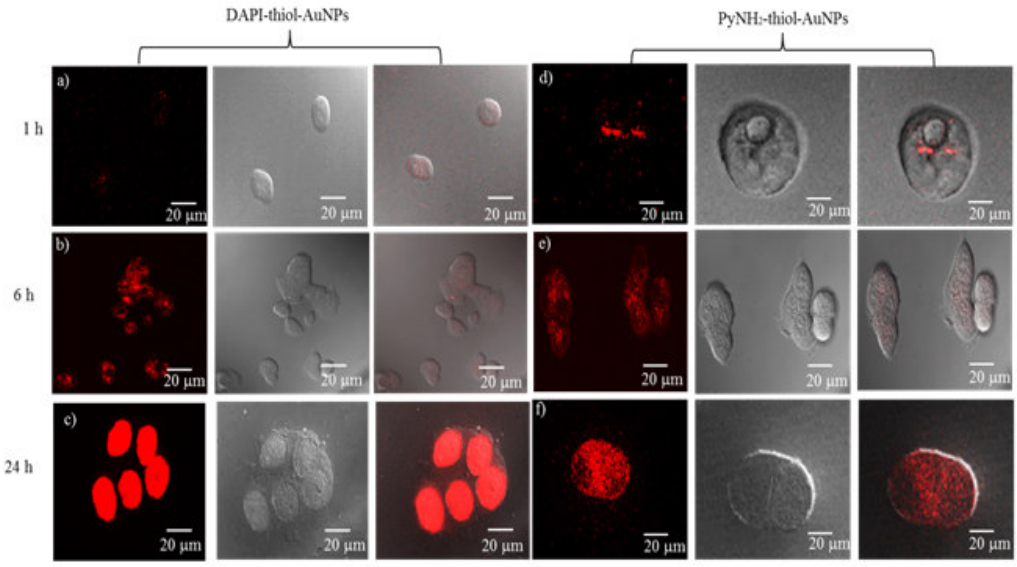

Figure 5

Fluorescence (left) (λ_{ex} = 405 nm, λ_{em} = 478), bright field (middle), and overlaid (right) images of T47D human breast cancer cells treated with DAPI-thiol-AuNPs or $pyNH_2$-thiol-AuNPs conjugates (a, d) after 1 h of incubation (b, e) after 6 h of incubation (c, f) after 24 h of incubation at room temperature.Original magnification was 63×.Scale bars = 20 µm.

TEM was used to support the results obtained from CLSM in relation to intercellular uptake and localization of AuNPs.TEM has been successfully used to recognize gold nanoparticles in thin sections of cells and to obtain high resolution images.[36] Gold nanoparticles appear as black spots in TEM due to their high atomic number.TEM analysis of the cells exposed to as prepared AuNPs or a fluorescence dye (DAPI or $pyNH_2$) loaded thiolated AuNPs for 3-4 h have shown an efficient internalization of AuNPs through cell membrane

(see Figure 6.a where the white arrows identify gold nanoparticles).To obtain detailed images of AuNPs internalized the cells, high magnification was applied.Cells treated with high concentrations of as prepared AuNPs or fluorescently labelled AuNPs conjugates (200 µL) were possibly taken up as groups of clusters.These clusters were found in the cytoplasmand were mainly localized in vacuoles (Figure 6.a).They were enclosed inside vesicles in cellular compartments (see Figure 6.a).

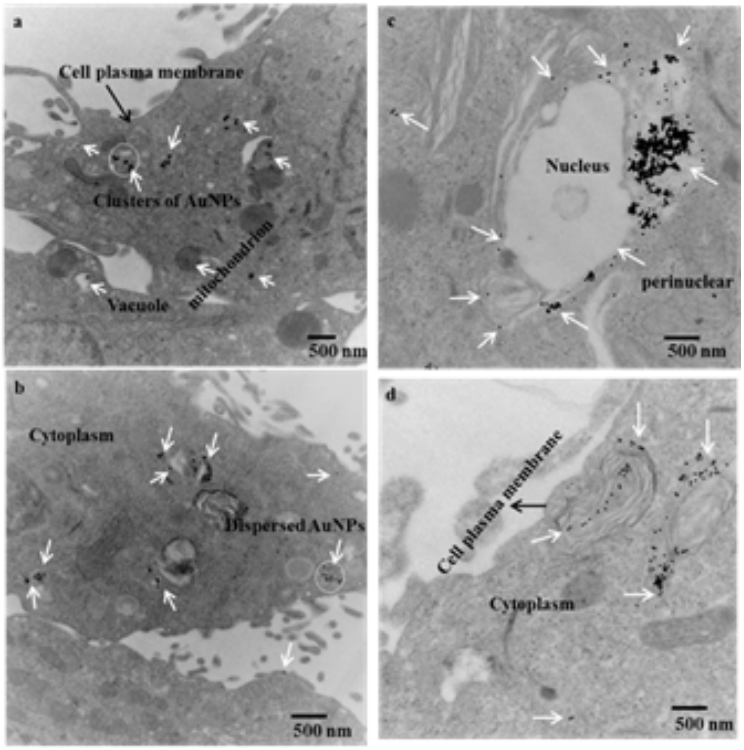

Figure 6

TEM images showing clusters and individual of AuNPs in cell cytoplasm of T47D cells exposed to 200 µL of (a& b) AuNPs (c) DAPI-thiol-AuNPs (d) pyNH$_2$-thiol-AuNPs (f) conjugates for 3-4 h.Scale bar = 500 nm.

DISCUSSION

Figure 2.A demonstrates the characteristic absorbance bands of free DAPI dissolved in Milli-Q water.Three main bands are observed.A clear and intense peak at 342 nm[37] and two weaker peaks at 261[38] and 225 nm were observed.The absorbance bands of DAPI-thiol-AuNPs are shown in Figure 2.A.A strong band observed at 343 nm was slightly shifted to the red compared to the unmodified DAPI.These results indicate the attachment of DAPI onto the functionalized AuNPs.The absorbance bands of pyNH$_2$-thiol-AuNPs conjugate are also shown in Figure 2.A and are very similar to that observed for free pyNH$_2$.Some absorption bands showed a slight shift to the red.The bands at 340 and 275 nm in free pyNH$_2$ showed a slight red shift in pyNH$_2$-thiol-AuNPs conjugate to be 341 and 276 nm, respectively.The red shift in this case can be attributed to the interactions between the –NH$_2$ group of pyNH$_2$with the –COOH groups of carboxylic acids terminated alkane-thiols on AuNPs and formation of amide group (O=C-NH).In addition, after attachment of pyNH$_2$ to thiol-AuNPs, the intense and sharp signals of pyNH$_2$ are still observed indicating the high absorbance of pyNH$_2$ after conjugation with thiol-AuNPs.This can be attributed to the fact that the pyNH$_2$ structures are far enough from AuNP due to the presence of the chains of alkane-thiols (16-MHDA and LA, used as linkers) to make the distance between the AuNPs and pyNH$_2$ molecules large enough to prevent any quenching.The SPR peak of the AuNPs is also red shifted in agreement with a study conducted by Ou et al.[31] In their study, carbon nanotube (CNT)-gold nanoparticle composites in aqueous solution using pyNH$_2$ as an interlinker were synthesized.They found that after functionalization of the AuNPs, the absorbance bands of pyNH$_2$ decreased and the SPR absorption peak of AuNPs was shifted to the red from 508 to 556 nm due to an interparticle plasmon coupling phenomenon.[31] In the current study, those observations indicate the attachment of amino functional group (–NH$_2$) of pyNH$_2$ with carboxylic ends of alkane-thiols functionalized AuNPs.A small red shift in theabsorption spectra was observed after attaching pyNH$_2$ onto thiol-AuNPs compared to unbound dye.These results are in agreement with a study reported by Basuet al.[33] They synthesized AuNPs in toluene using two-phases (water-toluene) in the presence of sodium borohydride as a reducing agent and a series of cationic surfactants.The fluorescence dye 1-methylaminopyrene (MAP) was used for the surface functionalization of the AuNPs.The emission bands at λ_{ex} = 328 nm were observed at 377, 397, and 417 nm.[33] The cytotoxicity results reveal the suitability of DAPI-thiol-AuNPs at any concentration tested to detect the cellular uptake and localization of AuNPs and suggesting use of this conjugate will be possiblefor other medical applications.However, the pyNH$_2$-thiol-AuNP conjugate can only be considered a safe product for intracellular applications when using very low concentrations.The CLSM results for free DAPI are in

agreement with other findings from other research groups.Manjiliet al.[39] used free DAPI to stain nuclei in MCF-7 breast cancer living cells.In that study the cells were incubated with DAPI for 24 h and DAPI stained the cells nuclei clearly.[39] Free $pyNH_2$ stained the cytoplasm but not the nuclei as shown in Figure 4.d.e and f.Low fluorescence was observed basically in cytoplasm and perinuclear region.No differences in fluorescence intensity were observed after longer periods of incubation (6 h and 24 h as shown in Figure 4.e and f).For the nanoparticles, after 1 h of incubation, low intensity fluorescence permeated throughout the membrane into the cytoplasm was observed in the cells (Figure 5 a, d).In the $pyNH_2$-thiol-AuNPs conjugate, most of the fluorescence accumulated in perinuclear region (Figure 5.d).After 6 h of exposure, a significant increase in intracellular fluorescence was observed in the conjugates containing DAPI or $pyNH_2$ dyes.The fluorescence was observed in all these conjugates in the cytoplasm, the cell periphery and near the perinuclear site (Figure 5.b and e).After 24 h incubation, intracellular fluorescence was more intense and distributed across the cells in contrast to that observed after 1 h or 6 h of treatment.The reason for this could be that some of the fluorescent dye molecules are disconnected from the AuNPs after long times in the cells.This allows some of free dye to enter the nuclei and stain them as clearly shown in Figure 5.c.The DAPI fluorescent probe, which was covalently attached to AuNPs through carboxylic acid terminated alkane thiol linkers, was used for CLSM to examine its behaviour as a probe when it is part of AuNPs.It was found that when DAPI conjugated to thiolated AuNPs, it did not behave same as when it was free.After conjugation, DAPI linked to thiolated AuNPs acted as a marker for AuNPs to detect their cellular uptake and internalization.It did not act as a nuclei stain as shown in Figure 5.a and b.These observations indicate that the DAPI on the AuNPs conjugate did not enter the nuclei as confirmed by TEM (Figure 6.b).However, when DAPI dissociates from the conjugate it could stain the nuclei.Images in Figure 5.a-f show the ability of all fluorescently labelled AuNPs conjugates to transport across the T47D cell membrane.This suggests that the interactions of T47D cells with AuNPs conjugates started very shortly after incubation and within an hour significant numbers of nanoparticles were internalized.This number significantly increased after 24 h.The confocal microscopy results for T47D living cells treated with DAPI-thiol-AuNPs or $pyNH_2$-thiol-AuNPs conjugates revealed an increase of intracellular fluorescence over time clearly showing the cellular uptake of gold nanoparticles.After 24 h, the particles seem to decompose into their constituents leading to different staining behaviour following the fluorophore's release (Figure 5.c and f).According to different reports AuNPs are internalized the cells via a receptor-mediated endocytosis mechanismand trapped in small vesicles known as endosomes.[40, 41] Then, those endosomes fuse with lysosomes for processing followed by transferring them to the cell periphery for excretion.[40, 41] Different studies have confirmed the presence of AuNPs inside various sections of the endocytic pathway including endosomes and lysosomes.[18, 41] It was hypothesized that large clusters were absorbed by plasma membrane and internalized the cells via endocytotic pathway due to the presence of AuNPs inside cells near the cell's membrane (Figure 6.b and d).The aggregation of AuNPs is governed by their surface chemistry.The chemical properties of AuNPs such as the surface characteristics and charge may change after mixing the AuNPs with the biological media due to non-selective absorption of serum proteins on the surface of AuNPs.Proteins attached onto the surface of AuNPs may improve the endocytotic pathway of the clustered AuNPs into the cells.[42] These findings are in agreement with other studies.[43, 44] For example, a study reported by Mustafa et al.[42] found that when exposing MC3T3-E1 osteoblastic cells to higher concentration (160 μg mL^{-1}) of AuNPs, the particles seem to internalize inside the cells mainly by an endocytosis mechanism with one or more pathways such as clathrin-and caveolae-mediated endocytosis, macropinocytosis, and pinocytosis.[42, 45] On the other hand, some AuNPs were found to be freely dispersed in the cell cytoplasm (Figure 6.b).These individual particles may internalize the cells by a diffusion process unlike phagocytosis and endocytosis mechanisms.Geiser et al.[46] investigated the possibility of nanomaterials passing through the plasma membrane and entering the cytoplasm by a non-phagocytic mechanism.[46] Rothen-Rutishauser et al.[47] found that 25 nm AuNPs and 22 nm titanium oxide nanoparticles may be internalized in the red blood cell membrane by a still unknown mechanism dissimilar to phagocytosis and endocytosis mechanisms.[47] However, the prime mechanism for internalization and penetration of AuNPs inside the cells is expected to be via endocytosis.The cellular uptake of AuNPs in DAPI-thiol-AuNPs conjugate was significantly higher than that for AuNPs without surface modifications (see Figure 6.c compared to Figure 6.a & b).This can be attributed to the ligand-receptor interactions in the cell membrane.[48] The electrostatic interactions between the positively charged surfaces of nanoparticles and the negatively charged cell plasma membrane can facilitate internalization the particles by cells.[49] Similar results have been reported by different groups.[50-52] For example, Harush-Frenkel et al.[51] investigated the difference of the endocytosis into HeLa cells of NPs having either a negative or positive charge on their surface.They found that the positively charged NPs internalized the cells rapidly via the clathrin-mediated pathway whereas the negatively charged NPs were internalized with low rate of endocytosis and did not use the clathrin-mediated endocytosis pathway.[51] The AuNPs in DAPI-thiol-AuNPs conjugate were localized in cytoplasm and near perinuclear region (see Figure 6.c).TEM data of T47D cells treated with $pyNH_2$-thiol-AuNPs conjugate shows the cellular uptake of AuNPs in these conjugates was low compared to DAPI-thiol-AuNPsconjugates (Figure 6.c and d) indicating the number of cationic groups (one for $pyNH_2$ versus two for DAPI) contributes to facilitating the internalization.The particles of $pyNH_2$-thiol-AuNPs conjugate were found near the cell's periphery and in the cytoplasm (see Figure 6.d).

CONCLUSION

DAPI and $pyNH_2$ dyes were covalently attached to the surface of gold nanoparticles through carboxylic terminated alkane thiols linkers and used as probes for intracellular internalization of AuNPs into T47D breast cancer cells.CLSM and TEM were used to track the conjugates.The results show that the particles were rapidly taken up by the cells via non-specific endocytosis and TEM imaging shows they are localized in cytoplasm, near the cell's internal membranes and in the perinuclear region.In addition, the conjugates show no cytotoxicity at most concentrations tested.Such dyes can be used for tracking other nanoparticles, following the fate of chemotherapy drugs in cells or assessing the heath of the cell nucleus in the case of DAPI.AuNPs functionalized with the dyes and antibodies could also be used for tumor detection.

CONFLICT OF INTEREST

The authors declare no conflicts of interest.

REFERENCES

1. Caruthers SD, Wickline SA, Lanza GM.Nanotechnological Applications in Medicine.Current Opinion in Biotechnology.2007; 18(1):26-30.
2. Fu W, Shenoy D, Li J, Crasto C, Jones G, Dimarzio C, et al.Biomedical Applications of Gold Nanoparticles Functionalized Using Hetero-bifunctional Poly (ethylene glycol) Spacer.DTIC Document, 2005.
3. Huang X, El-Sayed MA.Gold Nanoparticles: Optical Properties and Implementations in Cancer Diagnosis and Photothermal Therapy.Journal of Advanced Research.2010;1(1):13-28.
4. Ghosh P, Han G, De M, Kim CK, Rotello VM.Gold Nanoparticles in Delivery Applications.Advanced Drug Delivery Reviews.2008;60(11):1307-15.
5. Lakshmi VJ, Kannan, K.P.In vitro Evaluation of Antibiotic Conjugated Biogenic Gold Nanoparticles by Neosartorya Udagawae.International Journal of Pharma and Bio Sciences.2016;7(2):83 - 9.
6. Dykman LA, Khlebtsov NG.Uptake of Engineered Gold Nanoparticles into Mammalian Cells.Chemical Reviews.2014;114(2):1258-1288.
7. Gibson JD, Khanal BP, Zubarev ER.Paclitaxel-functionalized Gold Nanoparticles.Journal of the American Chemical Society.2007;129(37):11653-11661.
8. Shenoy D, Fu W, Li J, Crasto C, Jones G, DiMarzio C, et al.Surface Functionalization of Gold Nanoparticles using Hetero-bifunctional Poly(ethylene glycol) Spacer for Intracellular Tracking and Delivery.International journal of nanomedicine.2006;1(1):51-57.
9. Brust M, Walker M, Bethell D, Schiffrin DJ, Whyman R.Synthesis of Thiol-derivatised Gold Nanoparticles in a Two-phase Liquid-Liquid System.Journal of the Chemical Society, Chemical Communications.1994 (7):801-802.
10. Gao J, Huang X, Liu H, Zan F, Ren J.Colloidal Stability of Gold Nanoparticles Modified with Thiol Compounds: Bioconjugation and Application in Cancer Cell Imaging.Langmuir.2012;28(9):4464-4471.
11. Gupta RK, Srinivasan MP, Dharmarajan R.Synthesis of 16-Mercaptohexadecanoic Acid Capped Gold Nanoparticles and their Immobilization on a Substrate.Materials Letters.2012;67(1):315-319.
12. Rosi NL, Giljohann DA, Thaxton CS, Lytton-Jean AKR, Han MS, Mirkin CA.Oligonucleotide-Modified Gold Nanoparticles for Intracellular Gene Regulation.Science.2006;312(5776):1027-1030.
13. Dreaden EC, Austin LA, Mackey MA, El-Sayed MA.Size matters: Gold Nanoparticles in Targeted Cancer Drug Delivery.Therapeutic Delivery.2012;3(4):457-478.
14. Thanh NT, Green LA.Functionalisation of Nanoparticles for Biomedical Applications.Nano Today.2010;5(3):213-230.
15. Lin SY, Tsai YT, Chen CC, Lin CM, Chen CH.Two-step Functionalization of Neutral and Positively Charged Thiols onto Citrate-stabilized Au Nanoparticles.Journal of Physical Chemistry B.2004;108(7):2134-2139.
16. Tiwari PM, Vig K, Dennis VA, Singh SR.Functionalized Gold Nanoparticles and their Biomedical Applications.Nanomaterials.2011;1(1):31-63.
17. Lévy R, Shaheen U, Cesbron Y, Sée V.Gold Nanoparticles Delivery in Mammalian Live Cells: ACritical Review.Nano Reviews.2010;1:10.3402/nano.v1i0.4889.
18. Gonciar A.Detection of Intracellular Gold Nanoparticles.Biotechnology, Molecular Biology and Nanomedicine.2014;2(1):21-25.
19. Fan CH, Wang S, Hong JW, Bazan GC, Plaxco KW, Heeger AJ.Beyond Superquenching: Hyper-Efficient Energy Transfer from Conjugated Polymers to Gold Nanoparticles.Proceedings of the National Academy of Sciences of the United States of America.2003;100(11):6297-6301.
20. Degtyareva NN, Wallace BD, Bryant AR, Loo KM, Petty JT.Hydration Changes Accompanying the Binding of Minor Groove Ligands with DNA.Biophysical Journal.2007;92(3):959-965.
21. Kapuscinski J.DAPI - A DNA-specific Fluorescent Probe.Biotechnic & Histochemistry.1995;70(5):220-233.
22. Li M, Wu RS, Tsai JSC.DAPI Derivative: A fluorescent DNA Dye that Can be Covalently Attached to Biomolecules.Bioorganic & Medicinal Chemistry Letters.2003;13(24):4351-4354.
23. Rudershausen S, Grüttner C, Frank M, Teller J, Westphal F.Multifunctional Superparamagnetic Nanoparticles for Life Science Applications.European Cells and Materials.2002;3(supplement 2):81-83.
24. Yang X, Niu G, Cao X, Wen Y, Xiang R, Duan H, et al.The Preparation of Functionalized Graphene Oxide for Targeted Intracellular Delivery of siRNA.Journal of Materials Chemistry.2012;22(14):6649-6654.
25. Lodeiro C, Lima JC, Parola AJ, Seixas de Melo JS, Capelo JL, Covelo B, et al.Intramolecular Excimer Formation and Sensing Behavior of New Fluorimetric Probes and their Interactions with Metal Cations and Barbituric Acids.Sensors and Actuators B: Chemical.2006;115(1):276-286.

26. Kim DC, Kang DJ.Molecular Recognition and Specific Interactions for Biosensing Applications.Sensors.2008;8(10):6605-6641.
27. Grabar KC, Freeman RG, Hommer MB, Natan MJ.Preparation and Characterization of Au Colloid Monolayers.Analytical chemistry.1995;67(4):735-743.
28. Turkevich J, Stevenson PC, Hillier J.A Study of the Nucleation and Growth Processes in the Synthesis of Colloidal Gold.Discussions of the Faraday Society.1951;11:55-75.
29. Li D, He Q, Cui Y, Duan L, Li J.Immobilization of Glucose Oxidase onto Gold Nanoparticles with Enhanced Thermostability.Biochemical and Biophysical Research Communications.2007;355(2):488-493.
30. Yeh Y-C, Creran B, Rotello VM.Gold Nanoparticles: Preparation, Properties, and Applications in Bionanotechnology.Nanoscale.2012;4(6):1871-80.
31. Ou Y-Y, Huang MH.High-Density Assembly of Gold Nanoparticles on Multiwalled Carbon Nanotubes Using 1-Pyrenemethylamine as Interlinker.The Journal of Physical Chemistry B.2006;110(5):2031-2036.
32. Ding S-N, Cosnier S, Holzinger M, Wang X.Electrochemical Fabrication of Novel Fluorescent Polymeric Film: Poly(pyrrole–pyrene).Electrochemistry Communications.2008;10(10):1423-1426.
33. Praharaj S, Ghosh SK, Nath S, Kundu S, Panigrahi S, Basu S, et al.Size-Selective Synthesis and Stabilization of Gold Organosol in CnTAC: Enhanced Molecular Fluorescence from Gold-Bound Fluorophores.The Journal of Physical Chemistry B.2005;109(27):13166-13174.
34. Yejun Q, Jie Y, Jing Y, Cuili T, Xiaosong Z, Xuedong B, et al.Synthesis of Continuous Boron Nitride Nanofibers by Solution Coating Electrospun Template Fibers.Nanotechnology.2009;20(34):345603.
35. Worldwide MI.Dynamic Light Scattering Common Terms Defined http://www.malvern.com/en/ [cited 2016 6-04-2016].
36. Winkler J, Martin-Killias P, Pluckthun A, Zangemeister-Wittke U.EpCAM-targeted Delivery of Nanocomplexed siRNA to Tumor Cells with Designed Ankyrin Repeat Proteins.Molecular Cancer Therapeutics.2009;8(9):2674-2683.
37. Jung KS, Kim, M.,S., Lee, GJ, Cho, TS, Kim, S.K., Yi, S.Y.Conformation of Single Stranded poly(dA) and its Interaction with 4',6-diamidino-2-phenylindole.Bull Korean Chem Soc.1997;18(05): 510-514.
38. Kapuściński J, Szer W.Interactions of 4', 6-diamidine-2-phenylindole with Synthetic Polynucleotides.Nucleic Acids Research.1979;6(11):3519-3534.
39. Manjili HK, Ma'mani, L., Tavaddod, S., Mashhadikhan, M., Shafiee, A., Naderi-Manesh, H.D, L-sulforaphane Loaded Fe_3O_4@ Gold Core Shell Nanoparticles: APotential Sulforaphane Delivery System.PLOS ONE.2016; 11(3): e0151344.
40. Lim JP, Gleeson PA.Macropinocytosis: An Endocytic Pathway for Internalising Large Gulps.Immunol Cell Biol.2011;89(8):836-843.
41. Franzen S.A Comparison of Peptide and Folate Receptor Targeting of Cancer Cells: From Single Agent to Nanoparticle.Expert Opinion on Drug Delivery.2011;8(3):281-298.
42. Mustafa T, Watanabe, F., Monroe, W., Mahmood, M., Xu, Y., Saeed, L., M., Karmakar, A., Casciano, D., Ali, S., Biris, A., S.Impact of Gold Nanoparticle Concentration on their Cellular Uptake by MC3T3-E1 Mouse Osteoblastic Cells as Analyzed by Transmission Electron Microscopy.J Nanomedic Nanotechnol.2011;2(6):1000118.
43. Schaeublin NM, Braydich-Stolle LK, Maurer EI, Park K, MacCuspie RI, Afrooz ARMN, et al.Does Shape Matter? Bioeffects of Gold Nanomaterials in a Human Skin Cell Model.Langmuir.2012;28(6):3248-3258.
44. Geiser M, Quaile O, Wenk A, Wigge C, Eigeldinger-Berthou S, Hirn S, et al.Cellular Uptake and Localization of Inhaled Gold Nanoparticles in Lungs of Mice with Chronic Obstructive Pulmonary Disease.Particle and Fibre Toxicology.2013; 10:19.
45. Oh N, Park J-H.Endocytosis and Exocytosis of Nanoparticles in Mammalian Cells.International Journal of Nanomedicine.2014;9(Suppl 1):51-63.
46. Geiser M, Rothen-Rutishauser B, Kapp N, Schürch S, Kreyling W, Schulz H, et al.Ultrafine Particles Cross Cellular Membranes by Nonphagocytic Mechanisms in Lungs and in Cultured Cells.Environmental Health Perspectives.2005;113(11):1555-1560.
47. Rothen-Rutishauser BM, Schürch S, Haenni B, Kapp N, Gehr P.Interaction of Fine Particles and Nanoparticles with Red Blood Cells Visualized with Advanced Microscopic Techniques.Environmental Science & Technology.2006;40(14):4353-4359.
48. Bale SS, Kwon SJ, Shah DA, Banerjee A, Dordick JS, Kane RS.Nanoparticle-Mediated Cytoplasmic Delivery of Proteins To Target Cellular Machinery.ACS Nano.2010;4(3):1493-1500.
49. Wang J, Byrne JD, Napier ME, DeSimone JM.More Effective Nanomedicines through Particle Design.Small.2011;7(14):1919-1931.
50. Harush-Frenkel O, Altschuler Y, Benita S.Nanoparticle-cell Interactions: Drug Delivery Implications.Critical Reviews™ in Therapeutic Drug Carrier Systems.2008;25(6):485-544.
51. Harush-Frenkel O, Debotton N, Benita S, Altschuler Y.Targeting of Nanoparticles to the Clathrin-mediated Endocytic Pathway.Biochemical and Biophysical Research Communications.2007;353(1):26-32.
52. Harush-Frenkel O, Rozentur E, Benita S, Altschuler Y.Surface Charge of Nanoparticles Determines Their Endocytic and Transcytotic Pathway in Polarized MDCK Cells.Biomacromolecules.2008;9(2):435-443.